IOP Publishing Superconductor Science and Technology
Supercond. Sci. Technol. 31 (2018) 085009 (5pp) https://doi.org/10.1088/1361-6668/aad07d

Evidence for vortex splitting at the grain boundary in long $YBa_2Cu_3O_{7-\delta}$ grain boundary junctions

Tao Hua[1,2], Mei Yu[1], Haifeng Geng[1], Weiwei Xu[1], Yapeng Lu[1], Jianxin Shi[1], Weikang Shen[2], Jingbo Wu[1], Huabing Wang[1], Jian Chen[1] and Peiheng Wu[1]

[1] Research Institute of Superconductor Electronics, School of Electronic Science and Engineering, Nanjing University, Nanjing 210093, People's Republic of China
[2] School of Communication Engineering, Nanjing Institute of Technology, Nanjing 211167, People's Republic of China

E-mail: wwxu@nju.edu.cn

Received 11 March 2018, revised 20 June 2018
Accepted for publication 2 July 2018
Published 17 July 2018

Abstract

We investigated the current–voltage characteristics and the critical current density (J_c) of a $YBa_2Cu_3O_{7-\delta}$ grain boundary (GB) long Josephson junction with respect to magnetic field (H) under different application directions. When H is rotated within the bc-plane of the film, a small peak of J_c is observed when H is parallel to the c-axis, which denotes that there are some residual c-axis dislocations in the GB. When H is rotated within the ac-plane, some vortex-flow steps can be observed in the current–voltage curve at a high inclination angle of H. The vortex-flow step becomes smaller and wider with the decreasing angle between H and the c-axis. These results are a clear demonstration of vortex splitting at the GB plane in $YBa_2Cu_3O_{7-\delta}$ GB long Josephson junctions.

Keywords: vortex, high temperature superconductor, grain boundary

(Some figures may appear in colour only in the online journal)

1. Introduction

Due to the ultrashort coherence length (a few nanometers) and small critical current density (J_c) of polycrystalline samples of high critical temperature superconductors (HTS), the issue of interfaces is critical in terms of the fundamental physics and applications of HTS. Since polycrystalline HTS contain abundant complex grain boundaries (GBs), it is essential to study the properties of individual and well-defined interfaces. For this reason, bicrystal technology, possessing a single and well-defined GB, acts as an ideal way to analyze the transport properties of GBs. Generally, GBs can be classified according to the displacement and the rotation of the abutting crystals, where the displacement angle can be well controlled by the bicrystal substrates [1]. The superconducting critical current of HTS decreases at the GB, associated with the suppression of the superconducting order parameter. Recently, a considerable amount of theoretical and experimental work has been done towards understanding the fundamental behaviors of vortex motion along GBs [1–7]. Most of the relevant works are carried out where the magnetic field (H) is perpendicular to the plane of the superconducting film. In this case, all the vortices lie in the plane of the GB and the sample can be simplified as a two-dimensional (2D) system for the study of vortex transport. It has been demonstrated that the pinning force along the GB is much lower than that vertical to the GB [5–9]. This means that the GB can act as an easy-flow channel for vortex motion in HTS films [7–9].

When the applied magnetic field is tilted from the ab-plane, the issue of vortex motion will become more complicated. Once the magnetic field is along the out-of-plane GB, there can be vortex components along the GB plane in certain conditions [10, 11]. In particular, a vortex treading the HTS film can be split into two pinned vortex segments in the

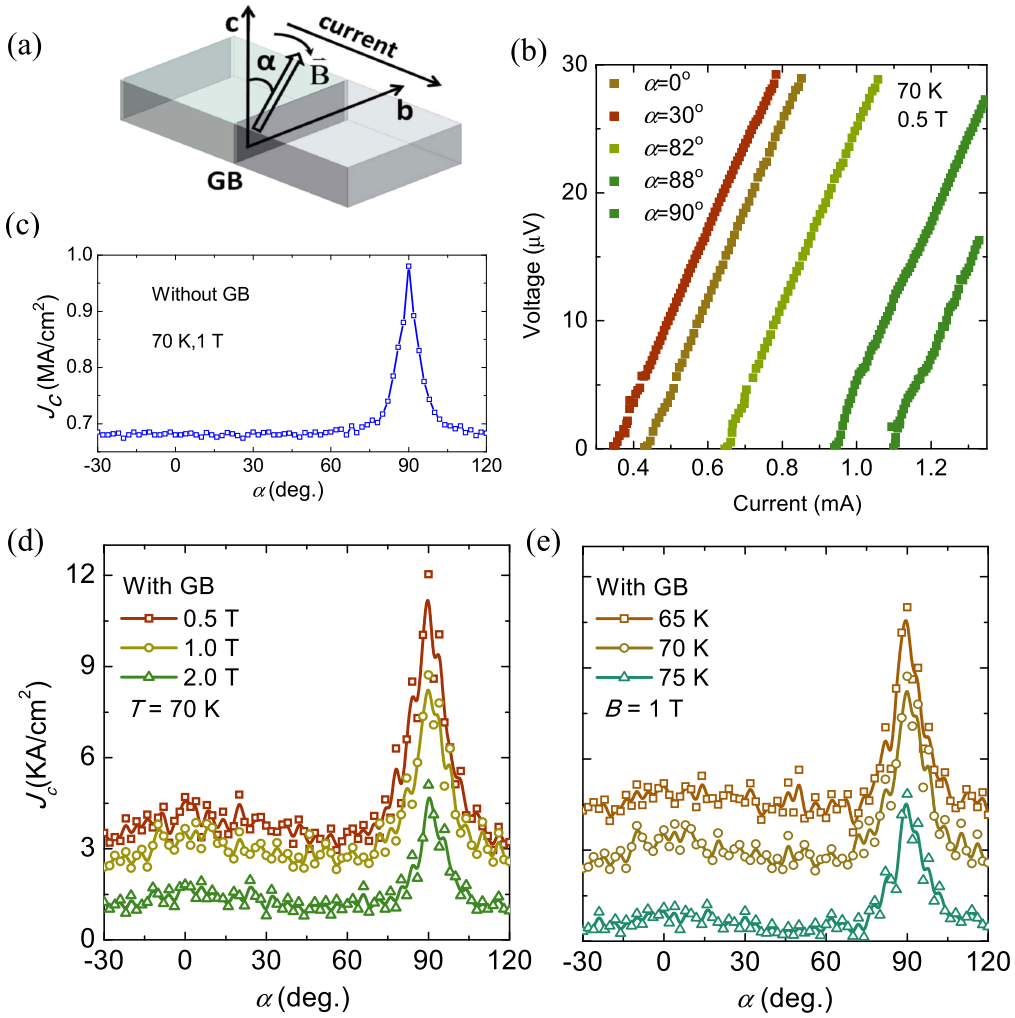

Figure 1. (a) The sketch of the sample and the measurement setup. The magnetic field is rotated in the *bc*-plane of the YBCO film. (b) The *I*–*V* characteristics of the YBCO microbridge with GBs for different α at $T = 70$ K and $\mu_0 H = 0.5$ T. For clarity, the superconducting state regions in *I*–*V* curves are not shown. (c) The measured J_c–α curve for the YBCO microbridge without GBs at $T = 70$ K and $\mu_0 H = 1$ T. (d) The measured J_c–α curves for the YBCO microbridge with GB at $T = 70$ K and $\mu_0 H = 0.5$ T, 1 T, 2 T. (e) The measured J_c–α curves for the YBCO microbridge with GB at $\mu_0 H = 1$ T and $T = 65$ K, 70 K, 75 K.

grains which are connected by a Josephson string in the GB plane. This vortex splitting or flux cutting effect has been intensively studied in HTS coated conductors with low angle GBs [10, 11]. By rotating the magnetic field and measuring the angular dependent J_c, the pinning potential across GBs in HTS coated conductors can be evaluated, and is found to be as large as that of heavy ion irradiated columnar defects [10].

In this paper, we studied the vortex motion and pinning behaviors of a long Josephson junction consisting of a microbridge structure with an $YBa_2Cu_3O_{7-\delta}$ (YBCO) bicrystal GB. The applied magnetic field was rotated within both the *bc*- and *ac*-plane of the film, respectively. The corresponding current–voltage (*I*–*V*) characteristics and J_c were measured with respect to the angle between the magnetic field and *c*-axis. We find the vortex splitting effect in the GB of YBCO bicrystal long Josephson junctions, for which the flux-flow behaviors are regarded as an important factor in determining the device performance [12–17].

2. Sample and setup

In our experiment, $YBa_2Cu_3O_{7-\delta}$ film with a thickness of 150 nm was deposited on a MgO bicrystal substrate (*c*-axis (001) orientation) using the physical vapor deposition method. The zero-field J_c of the film without a GB was 3.8 MA cm^{-2} at 77 K, and the measured zero-resistance temperature of a GB-free film microbridge was 86.2 K at zero magnetic field. The MgO bicrystals were formed by hot pressing two single crystals with the same configuration of [001] but with a 24° tilt angle. The bicrystal substrate with a misorientation angle of 24° results in the formation of a GB in YBCO film during the its epitaxial growth process. The structure of the YBCO microbridge across a GB was patterned using conventional photolithography and ion beam milling.

As shown in figure 1(a), the GB is perpendicular to the microbridge, and the width of the microbridge is 60 μm. The sample can be viewed as a long bicrystal Josephson junction,

since the junction length (60 μm) is much larger than the Josephson penetration depth (λ_J). The λ_J can be calculated by $\lambda_J = (\Phi_0/2\pi\mu_0 J_c d)^{1/2}$, where Φ_0 is the magnetic flux quantum, μ_0 is the vacuum permeability, J_c is the critical current density, and d is the effective magnetic thickness of the junction, which is about two times the London penetration depth (λ_L). For the HTS GB junction, λ_J at the temperature of liquid nitrogen is generally in the order of 1 μm. The transport measurement was performed using a Physical Property Measurement System (PPMS-9). The sample was located onto a rotatable platform with an adjustable DC magnetic field that was originally oriented along the c-axis. The sample temperature (T) could be slowly swept at the rate of 0.015 K s^{-1}, and the drive current could be swept at the rate of 10 μA s^{-1}.

3. Experiments and results

Firstly, we rotated the applied magnetic field in the bc-plane of the film, as displayed in figure 1(a). Here, the value of α denotes the angle between H and the c-axis of the film. The DC current was applied along the a-axis, i.e., the induced current was always perpendicular to the GB. In this case, the vortices can lie wholly in and be rotated inside the plane of the GB. Figure 1(b) shows the I–V characteristics for different α at $T = 70$ K and $\mu_0 H = 0.5$ T. Figure 1(d) shows the angular dependence of J_c at $T = 70$ K for $\mu_0 H$ of 0.5 T, 1 T, and 2 T, while figure 1(e) shows the angular dependence of J_c at $\mu_0 H = 1$ T for $T = 65$ K, 70 K, and 75 K.

For comparison, the magnetic field angle dependence of J_c of a microbridge without a GB was also studied. Figure 1(c) shows the J_c–α curve at 70 K under a magnetic field of 1 T. The maximum J_c is found to be ~0.95 MA cm^{-2} at the angle of 90°, namely, along the b-axis of the film. It seems there is an angular-independent profile at angle from −30° to 60°, which is consistent with the previous results [18, 19].

By comparing the magnetic field angular dependence of J_c of the YBCO microbridges with and without GBs, we find that: (a) the J_c of the microbridge with GB is about two orders of magnitude less than that of the GB-free one; (b) the sharp peaks at $\alpha = 90°$ are observed in the J_c–α curves of the microbridges regardless of whether there is a GB or not; (c) the microbridge with a GB demonstrates a wide statistical peak at $\alpha = 0°$ on the J_c–α curves, while such a peak is absent for the GB-free sample.

In general, the J_c–α curve of a HTS film can be strongly affected by the anisotropic vortex pinning. The peak of the J_c–α curve for a magnetic field aligned with the plane of the HTS film was often called the intrinsic pinning peak. It originated from the intrinsic pinning effects in the ab-plane of the [001] oriented HTS film due to its 2D crystal structure [10, 18]. Indeed, sharp peaks of J_c are shown for both of our two YBCO microbridges at $\alpha = 90°$, i.e., the magnetic field is aligned with the b-axis of the film.

On the other hand, in HTS films, the peak of the J_c–α curves at $\alpha = 0°$, i.e., when the magnetic field is aligned with the c-axis, was often induced by the c-axis correlated pinning

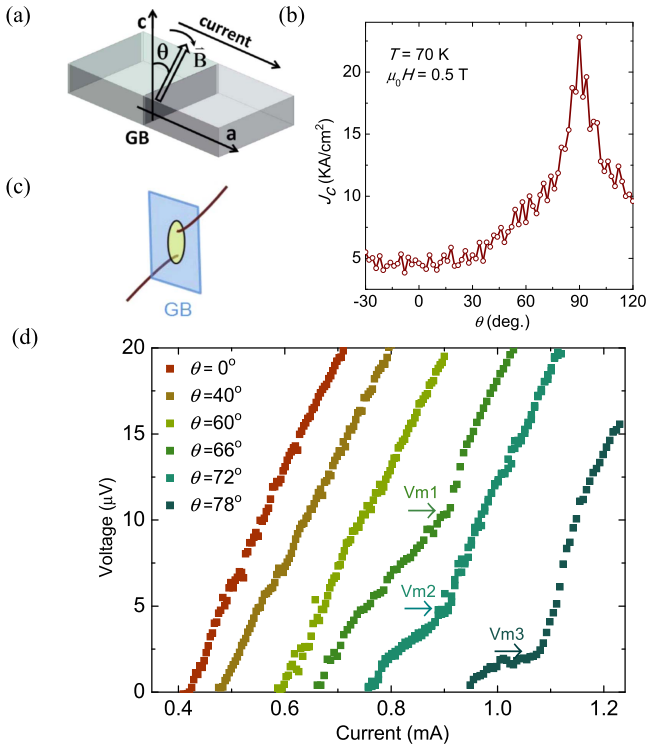

Figure 2. (a) The sketch of the sample and the measurement setup. The magnetic field is rotated in the ac-plane of the film. (b) The J_c–θ curve for the YBCO microbridge with the GB at $T = 70$ K and $\mu_0 H = 0.5$ T. (c) The sketch of a Josephson vortex component along the GB plane. (d) The measured I–V characteristics of the YBCO microbridge with the GB for different θ at $T = 70$ K and $\mu_0 H = 0.5$ T. For clarity, superconducting state regions in I–V curves are not displayed. The horizontal arrows (step voltage V_{m1}, V_{m2}, and V_{m3}) mark the peaks of the steps with different θ.

centers in HTS films, such as dislocations, nanorods, nanoparticles, and so on [20, 21]. It was found that the low angle GBs in HTS coated conductors consist of a lot of dislocations along the c-axis, which lead to a remarkable peak at $\alpha = 0°$ in the J_c–α curves [18, 19]. In the measured J_c–α curve of the YBCO microbridge with a 24° GB, the peak at $\alpha = 0°$ for different $\mu_0 H$ and T is still noticeable, though the value is relatively small. It suggests that there are still some residual c-axis dislocations in our 24° GB, although most of the dislocations in the GB are very close and are merged into a closed interface layer section.

In the following, we rotated the applied magnetic field in the ac-plane of the microbridge with a GB as shown in figure 2(a), and measured the I–V characteristics for various angles (θ) between the magnetic field and c-axis. Figure 2(d) shows I–V curves for different angles at $\mu_0 H = 0.5$ T and a temperature of 70 K with a DC current applied along the a-axis. In this case, although the GB is still a high power-dissipation channel, the vortices can diagonally cross the plane of the GB.

Figure 2(b) shows the J_c–θ curve for the microbridge with the GB at $T = 70$ K and $\mu_0 H = 0.5$ T. With the increase of θ, the value of J_c rises, and the growth rate of J_c with θ also rises. There is also a peak in the J_c–θ curve at $\theta = 90°$, such

phenomena are similar to the pure film bridge without a GB [10]. However, the J_c of the GB sample is always smaller than that of the film sample without a GB regardless of the values of θ. The peaks at $\theta = 90°$ can be attributed to the intrinsic pinning in the *ab*-plane of the [001] oriented YBCO film.

It is interesting that some resonance-like steps in the *I*–*V* curves can be clearly observed for a relatively large value of θ ($\theta > 66°$ in figure 2(d)). Here we denote the voltage value at the step as the step voltage (V_m). As θ decreases, V_m increases, and the step becomes wider, meanwhile, the height of the step gradually decreases. We relate these steps to the flux-flow (velocity matching) steps, as the height and the scope of the steps obey the same monotonically decreasing relationship [15, 22–28]. The appearance of flux-flow steps for long GB junctions is due to the continuous Josephson vortex flow in the GB plane [22–28]. In previous studies, there has been a research into the vortex-flow steps that appeared in the *I*–*V* curves of long Josephson junctions such as low-T_c superconductor–insulator–superconductor long junctions, low-T_c superconductor–normal conductor–superconductor long junctions, and high-T_c GB long junctions [22–31]. However, all of these works were limited to the example where the magnetic field is along the *c*-axis of the superconducting film. The physical origins of *I*–*V* vortex-flow steps can be explained as follows. The DC current, producing a Lorentz force, drives the Josephson vortices moving continuously along the junction plane with a velocity of u. Meanwhile, based on the theory in [15, 28], the electromagnetic wave can propagate along the junction with a phase velocity (Swihart velocity) of v. When u approaches v, the resonance is excited and a step appears.

Since the origin of *I*–*V* resonance-like steps is the flow of Josepshon vortices along the GB, our experimental results imply that there still can be Josephson vortex components flowing inside the plane of the GB though the vortices diagonally crossing the GB, which is in agreement with the model that a vortex can be cut by a GB into two vortex components in the HTS grains, where the grains are connected by a Josephson component in the GB plane, as depicted in figure 2(c). In this vortex system, the superconducting critical current (I_c) is determined by the onset of flux cutting. As the applied current reaches I_c and beyond, the components of the Josephson vortex in the GB plane start flowing, which results in the appearance of the *I*–*V* resonance-like steps.

For our YBCO GB junction, there is almost no hysteretic behavior in the *I*–*V* curves at different T without a magnetic field (the data is not shown here), which indicates our sample is overdamped and its Stewart–McCumber parameter (β_c) is below 1. Generally, the vortex-flow *I*–*V* steps in overdamped long junctions are not so steep as those in underdamped long junctions, such as $Nb/AlO_x/Nb$ junctions [29, 30]. Indeed, when $\theta < 66°$, the height of the step is too small to be observed. When $\theta > 84°$, the scope of the step becomes very narrow, and the V_m is very small. As a result, the step is difficult to recognize.

Based on previous theoretical work, V_m is approximately linear with the applied magnetic field when the magnetic field is along the *c*-axis [15, 28]. The V_m can be calculated by $V_m = FduB_e$ [15], where F is the flux focusing factor, B_e is the vertical magnetic field, and d is the effective magnetic thickness and is equal to $d \approx 2\lambda_L$. As for the Swihart velocity, $u = c_0(t/\varepsilon_r d)^{1/2}$, where c_0 is the velocity of light, t is the barrier (boundary) thickness, and ε_r is the relative dielectric constant of the grains of YBCO. Since V_m is proportional to the magnetic field along the *c*-axis and the *c*-axis magnetic field results in the vortices lying in the plane of the GB, V_m is nearly proportional to the equivalent magnetic field of the Josephson vortex components along the *c*-axis in the GB plane when the magnetic field is rotated within the *ac*-plane. In our results, as shown in figure 2(d), the value of V_m decreases with the increase of θ. Correspondingly, the GB *c*-axis Josephson vortex components decrease with increasing θ. It is noted that the equivalent magnetic field of the *c*-axis Josephson vortex components is much smaller than the *c*-axis component of the inclined magnetic field ($\mu_0 H\cos\theta$), and $\mu_0 H\cos\theta$ also decreases with the increase in θ. By calculating the values of $(V_{m\theta 1} - V_{m\theta 2})/(\cos\theta_1 - \cos\theta_2)$, we can compare the decrease rate of both the *c*-axis Josephson vortex components and $\mu_0 H\cos\theta$ relative to θ. From figure 2(d) we can find that the value of $(V_{m1} - V_{m2})/(\cos 66° - \cos 72°)$ is significantly larger than the value of $(V_{m2} - V_{m3})/(\cos 72° - \cos 78°)$, which denotes that the decrease rate of the GB *c*-axis Josephson vortex components relative to θ is higher than the cosine law, i.e. the decrease rate of the *c*-axis component of magnetic field relative to θ. Furthermore, if we define an equivalent vertical magnetic field B_e' to match the GB *c*-axis Josephson vortex components, using the formula of V_m and the values of the parameters for a typical YBCO long GB junction in [15] ($F \approx 10$, $d \approx 280$ nm, and $t/\varepsilon_r \approx 0.2$ nm), we can reveal that the estimated B_e' is in the order of 10^{-2} Gauss.

4. Conclusion

We investigated the *I*–*V* characteristics and the magnetic field angular dependence of J_c for YBCO bridges with a bicrystal GB at different magnetic fields. As the magnetic field is rotated within the *bc*-plane of the film, a sharp peak at $\alpha = 90°$ is exhibited in the J_c–α curves and there is an unremarkable peak at $\alpha = 0°$ regardless of T and H. The peak at $\alpha = 90°$ is caused by the intrinsic pinning in the *ab*-plane of the [001] oriented YBCO film, while the peak at $\alpha = 0°$ is caused by the residual *c*-axis dislocations in the GB. As the magnetic field is rotated within the *ac*-plane of the film, vortex-flow resonance steps were observed in the *I*–*V* curves when $66° < \theta < 84°$. These results provide evidence of vortex splitting at the bicrystal GB plane in YBCO long GB Josephson junctions. This vortex-flow step becomes bigger and narrower with increasing θ, suggesting that the Josephson vortex components in the GB plane decrease with increasing θ.

Acknowledgments

This work was supported by the National Natural Science Foundation of China (61501222, 61571219, 61727805, and 61701219), the National Key R&D Program of China (2016YFA0301801) and Jiangsu Provincial Natural Science Fund (BK20170649). Also, it was partially supported by the Fundamental Research Funds for the Central Universities, Innovative Research Team in University (PCSIRT) and Jiangsu Key Laboratory of Advanced Techniques for Manipulating Electromagnetic Waves. The authors thank Professor Jun Li for his critical reading and revision suggestions for the manuscript.

ORCID iDs

Tao Hua https://orcid.org/0000-0002-7737-0195
Huabing Wang https://orcid.org/0000-0003-4802-6077
Jian Chen https://orcid.org/0000-0002-1360-8969

References

[1] Hilgenkamp H and Mannhart J 2002 *Rev. Mod. Phys.* **74** 485
[2] Gurevich A and Ciovati G 2008 *Phys. Rev.* B **77** 104501
[3] Durrell J H and Rutter N A 2009 *Supercond. Sci. Technol.* **22** 013001
[4] Rouco V, Palau A and Guzman R 2014 *Supercond. Sci. Technol.* **27** 125009
[5] Horide T, Matsumoto K, Ichinose A, Mukaida M, Yoshida Y and Horii S 2007 *Phys. Rev.* B **75** 020504
[6] Verebelyi D T *et al* 2000 *Appl. Phys. Lett.* **76** 1755
[7] Hogg M J, Kahlmann F, Tarte E J, Barber Z H and Evetts J E 2001 *Appl. Phys. Lett.* **78** 1433
[8] Zhu B Y, Dong J M, Xing D Y and Zhao B R 1998 *Phys. Rev.* B **57** 5075
[9] Hua T *et al* 2015 *Supercond. Sci. Technol.* **28** 025005
[10] Horide T and Matsumoto K 2012 *Appl. Phys. Lett.* **101** 112604
[11] Durrell J H, Hogg M J, Kahlmann F, Barber Z H, Blamire M G and Evetts J E 2003 *Phys. Rev. Lett.* **90** 247006
[12] Jaworski M 2008 *Supercond. Sci. Technol.* **21** 065016
[13] Revin L S, Pankratov A L, Chiginev A V, Masterov D V, Parafin A E and Pavlov S A 2018 *Supercond. Sci. Technol.* **31** 045002
[14] Winkler D, Zhang Y M, Nilsson P A, Stepantsov E A and Claeson T 1994 *Phys. Rev. Lett.* **72** 1260
[15] Zhang Y M, Winkler D, Nilsson P-A and Claeson T 1995 *Phys. Rev.* B **51** 8684
[16] Sung H H, Yang S Y, Horng H E and Yang H C 1999 *IEEE Trans. Appl. Supercond.* **9** 3937
[17] Katterwe S O and Krasnov V M 2011 *Phys. Rev.* B **84** 214519
[18] Diaz A, Mechin L, Berghuis P and Evetts J E 1998 *Phys. Rev. Lett.* **80** 3855
[19] Horide T, Matsumoto K, Yoshida Y, Mukaida M, Ichinose A and Horii S 2007 *Physica* C **463** 678
[20] Dam B *et al* 1999 *Nature* **399** 439
[21] Civale L 1997 *Supercond. Sci. Technol.* **10** A11
[22] Masterov D V, Parafin A E, Revin L S, Chiginev A V, Skorokhodov E V, Yunin P A and Pankratov A L 2017 *Supercond. Sci. Technol.* **30** 025007
[23] Guillaume A, Scholtyssek J M, Brendel C, Ludwig F and Schilling M 2012 *Phys. Proc.* **36** 19–24
[24] Revin L S, Chiginev A V, Pankratov A L, Masterov D V, Parafin A E, Luchinin G A, Matrozova E A and Kuzmin L S 2013 *J. Appl. Phys.* **114** 243903
[25] Chesca B, John D and Mellor C J 2014 *Supercond. Sci. Technol.* **27** 055019
[26] Kupriyanov M Y, Khapaev M M, Divin Y Y and Gubankov V N 2012 *JETP Lett.* **95** 289
[27] Navacerrada M A, Lucia M L and Sanchez-Quesada F 2012 *Physica* C **483** 195
[28] Swihard J C 1961 *J. Appl. Phys.* **32** 461
[29] Zhang Y M, Winkler D and Claeson T 1993 *Appl. Phys. Lett.* **62** 3195
[30] Pankratov A L, Sobolev A S, Koshelets V P and Mygind J 2007 *Phys. Rev.* B **75** 184516
[31] Mezzetti E, Gerbaldo R, Ghigo G, Gozzelino L, Minetti B, Camerlingo C, Monaco A, Cuttone G and Rovelli A 1999 *Phys. Rev.* B **60** 7623